Approximative Model Reconstruction of Cascade Systems

Henrik Sandberg[a,*], Per Hägg[a], Bo Wahlberg[a]

[a] *Automatic Control Lab, ACCESS Linnaeus Center, School of Electrical Engineering, KTH Royal Institute of Technology, SE-100 44 Stockholm, Sweden.*

Abstract

This letter considers how to approximately reconstruct a cascade system from a given unstructured system estimate. Many system identification methods, including subspace methods, provide reliable but generally unstructured black-box models. The problem we consider is how to find cascade systems that are close to such black-box models. For this, we use model matching techniques and optimal weighted Hankel-norm approximation to obtain accurate low-order cascade systems. We show that it is possible to bound the reconstruction error in terms of an error tolerance parameter and weighted Hankel singular values. The suggested methods are illustrated on both a numerical example and a real double tank system with experimental data.

Keywords: model reduction, cascade systems, model matching

1. Introduction

Consider the block diagram in Figure 1. In Subfigure (a), we have a parallel connection of two linear systems H_1 and H_2, and in Subfigure (b) we have a cascade of the linear systems G_1, G_2, F_1, and F_2. System identification often results in models without particular interconnection structures, *i.e.* systems of the type H_1 and H_2, which can model any linear system with one input and two outputs. Nevertheless, it is common that real physical systems have a cascade-like structure, such as the one in Subfigure 1-(b).

*Corresponding author. Tel.: +46 87907294; fax: +46 87907329.

Email addresses: hsan@kth.se (Henrik Sandberg), pehagg@kth.se (Per Hägg), bo@kth.se (Bo Wahlberg)

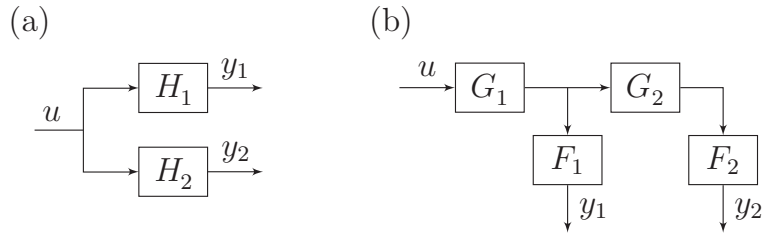

Figure 1: The parallel connection of the linear systems H_1 and H_2 in (a) can model any linear system with one input and two outputs. The goal of this letter is to develop techniques that match the cascade of linear subsystems G_1 and G_2, for given F_1 and F_2, in (b) to the given unstructured system in (a).

For example, as we shall study closer in Section 5.2, in a series connection of fluid tanks the output flow of the first tank goes into the second tank. There are numerous similar examples in process industry.

The objective of this letter is to determine subsystems G_1 and G_2, given H_1, H_2, F_1, and F_2, such that the mapping $u \mapsto (y_1, y_2)$ is well preserved. We assume the filters F_1 and F_2 are *known*, along with the unstructured system estimate H_1 and H_2. The filters F_1 and F_2 may model known anti-aliasing filters, as an example. In practice, the systems H_1 and H_2 could be obtained from black-box system identification, using prediction error methods or subspace methods [1], for instance.

Note that it is not straightforward to obtain low-order and stable subsystems G_1 and G_2 from the given systems, since methods based on simple division may result in unstable, inaccurate, and high-order solutions. The techniques we use to solve the problem exploit methods from robust control (model matching [2]) and model reduction (optimal weighted Hankel-norm approximation [3, 4, 5, 6]), and ensure that stable and close-to-optimal subsystems G_1 and G_2 are found. One of the first ideas of using model reduction in system identification is [7]. A more recent study is [8]. The general result is that it is best to first estimate a high-order model, which gives a good description of the true system, and then in a second step approximate this model with a reduced-order one. However, there seem to be few results on how to find reduced-order models with specific structures, and in particular without using non-convex numerical optimization methods. Finally note

that the methods presented herein to solve the problem could be generalized to cascades of more than two systems. We will also only consider SISO (Single-Input–Single-Output) systems H_1, H_2, G_1, G_2, F_1, and F_2, but the results may be extended to multi-dimensional systems.

The outline of the letter is as follows. The detailed problem formulation is given in Section 2. In Section 3, we construct high-order cascade systems that match the given unstructured system. In Section 4, it is shown how model reduction can be used to obtain low-order and high-quality subsystems G_1 and G_2. The methods are then applied to a numerical and a real example with experimental data in Section 5. In Section 6, we state some theoretical results concerning the convergence properties of the presented methods. The conclusions are given in Section 7. The proofs are found in the appendix. This letter significantly extends the work presented in [9].

Notation

We consider linear discrete-time systems G with real rational transfer matrices $G(z)$, $z \in \mathbb{C}$. For convenience, we often identify the system with its transfer matrix. By $\deg G$ we mean the order of a minimal realization of $G(z)$, and we use $G(z)^\sim := [G(1/z)]^T$. To measure the system G we use the $\mathcal{L}_\infty$-norm $\|G\|_\infty := \sup_\omega \bar{\sigma}(G(e^{j\omega}))$ ($\bar{\sigma}$ is the largest singular value), and the $\mathcal{L}_2$-norm $\|G\|_2 := (1/\sqrt{2\pi}) \left(\int_{-\pi}^{\pi} \mathrm{trace}[G(e^{j\omega})^\sim G(e^{j\omega})]\, d\omega \right)^{1/2}$. Let $\mathbb{D}_a$ be an open disc in the complex plane, $\mathbb{D}_a := \{z \in \mathbb{C} : |z| < a\}$, and $\mathbb{C}_a := \mathbb{C} \setminus \bar{\mathbb{D}}_a = \{z \in \mathbb{C} : |z| > a\}$. By $\mathcal{RH}_\infty(\mathbb{C}_a)$ ($\mathcal{RH}_\infty^-(\mathbb{C}_a)$) we mean the set of real rational transfer matrices which are analytic and bounded in the set $\mathbb{C}_a$ ($\mathbb{D}_a$). Often $a = 1$, and we then simply write $\mathcal{RH}_\infty$ ($\mathcal{RH}_\infty^-$). A system G with real rational transfer matrix is (input-output) stable if, and only if, $G(z) \in \mathcal{RH}_\infty$. By $\mathcal{RH}_\infty^-(r)$ we mean the set of real rational transfer matrices which can be decomposed as $G(z) = G_s(z) + G_u(z)$ where $G_u(z) \in \mathcal{RH}_\infty^-$ and $G_s(z) \in \mathcal{RH}_\infty$ and $\deg G_s \leq r$.

2. Problem Formulation

Consider again the two block diagrams in Figure 1. The problem we study in this letter is to systematically determine low-order SISO subsystems $G_1, G_2 \in \mathcal{RH}_\infty$ of a cascade, such that the $\mathcal{L}_\infty$-norm approximation error

$$\gamma(G_1, G_2) := \left\| \begin{bmatrix} \lambda_1(H_1 - F_1 G_1) \\ \lambda_2(H_2 - F_2 G_2 G_1) \end{bmatrix} \right\|_\infty \tag{1}$$

is small. Here the SISO systems $H_1, H_2 \in \mathcal{RH}_\infty$ are given, and we sometimes say they are models of the first and second channel of the system. We also use the notation $H = \begin{bmatrix} H_1 & H_2 \end{bmatrix}^T$. The SISO systems $F_1, F_2 \in \mathcal{RH}_\infty$ and $\lambda_1, \lambda_2 \in \mathcal{RH}_\infty$ are also given, possibly frequency-dependent filters and weights, respectively. The additional degrees of freedom offered by the weights λ_1 and λ_2 can be used to improve the approximation accuracy over certain frequency ranges. We summarize the assumptions on the given systems next.

Assumption 1. *$H_1, H_2, F_1, F_2, \lambda_1, \lambda_2 \in \mathcal{RH}_\infty$, and F_1, F_2, λ_1, and λ_2 have no zeros on the unit circle ($|z| = 1$).*

The assumption of no zeros on the unit circle will be used to derive error bounds in the following. If it is not fulfilled for the given systems, one can apply a small perturbation to remove those zeros.

As discussed in Section 1, we can assume some standard modeling tool, such as system identification, has been used to determine the systems H_1 and H_2 in Figure 1–(a). In general, it is not possible to exactly factorize H_1 and H_2 into a cascade form, see Figure 1–(b). In order for the studied problem to make sense, however, we do need to assume that there indeed exists a cascade system close to H. We introduce a reconstruction error parameter $\epsilon > 0$, which is given and quantifies that there is a cascade system in the ϵ-neighborhood of H, as formalized in the following assumption.

Assumption 2. *For given $\epsilon > 0$, there are subsystems $G_1, G_2 \in \mathcal{RH}_\infty$ such that $\gamma(G_1, G_2) \leq \epsilon$. Let the subsystems $G_1^\star, G_2^\star \in \mathcal{RH}_\infty$ of orders $n_1^\star$ and $n_2^\star$, respectively, be subsystems of lowest possible total order $n_1^\star + n_2^\star$ such that $\gamma(G_1^\star, G_2^\star) \leq \epsilon$.*

We may think of $G_1^\star$ and $G_2^\star$ as "ideal" solutions to the reconstruction problem. They are the lowest-order subsystems in the ϵ-neighborhood of H. However, they may be hard to find, since that involves non-convex optimization as further discussed in Section 3. In the following sections, we will therefore develop tractable methods for how to find reasonable values for ϵ, and how to find subsystem G_1 and G_2 inside, or close to, the ϵ-neighborhood. We will also see how to find estimates of the lowest possible orders $n_1^\star$ and $n_2^\star$.

3. Finding a Cascade-Structured System

Given the system H, satisfying Assumptions 1–2, how can we find a cascade of subsystems $\hat{G}_1$ and $\hat{G}_2$ such that the error $\gamma(\hat{G}_1, \hat{G}_2)$ is small? Any method involving inversion of the known transfer functions H_1, H_2, F_1, F_2, λ_1, or λ_2, should be avoided since it may result in unstable or acausal subsystems. In this section, we provide a partial solution based on model matching techniques. The reason the subsystems are denoted $\hat{G}_1$ and $\hat{G}_2$ is that they are considered preliminary in that we are here only concerned with their reconstruction error, and not their model order. How to systematically reduce their orders is postponed until Section 4.

To find a stable and accurate cascade system, we first propose to estimate the model orders n_1 and n_2 using physical insight or other prior information, and to solve the optimization problem

$$(\hat{G}_1^\star, \hat{G}_2^\star) := \arg \min_{\substack{\hat{G}_1, \hat{G}_2 \in \mathcal{RH}_\infty \\ \deg \hat{G}_1 \le n_1, \deg \hat{G}_2 \le n_2}} \gamma(\hat{G}_1, \hat{G}_2). \tag{2}$$

Since (2) is a non-convex optimization problem if $\lambda_2 F_2 \neq 0$, the optimization is generally non-trivial. Nevertheless, efficient sub-gradient methods that converge to local minima of (2) are available [10]. For example, one can readily use the command `hinfstruct` in MATLAB [11]. However, choosing a good starting point for the optimization, and suitable model orders n_1 and n_2 may be non-trivial. These problems are further discussed in Section 5. If we can verify that the global optimum $\hat{G}_1^\star$ and $\hat{G}_2^\star$ was found and the chosen orders were high enough, the following bound on reconstruction error of course holds.

Proposition 1. *Suppose Assumptions 1–2 hold, $n_1 \ge n_1^\star$, and $n_2 \ge n_2^\star$. Then $\hat{G}_1^\star$ and $\hat{G}_2^\star$ satisfy $\gamma(\hat{G}_1^\star, \hat{G}_2^\star) \le \epsilon$.*

Since $\hat{G}_1^\star$ and $\hat{G}_2^\star$ may be hard to determine, we propose a convex relaxation of the optimization problem (2) next, ignoring the order constraints. Let us study a recursion of simpler quasi-convex $\mathcal{H}_\infty$ model matching problems [2], indexed by the integer $k \ge 0$,

$$\begin{aligned} \hat{G}_1^{(k+1)} &:= \arg \min_{\hat{G}_1 \in \mathcal{RH}_\infty} \gamma(\hat{G}_1, \hat{G}_2^{(k)}) \\ \hat{G}_2^{(k+1)} &:= \arg \min_{\hat{G}_2 \in \mathcal{RH}_\infty} \gamma(\hat{G}_1^{(k+1)}, \hat{G}_2), \end{aligned} \tag{3}$$

where $\hat{G}_1^{(0)}$ and $\hat{G}_2^{(0)}$ are some initial estimates of G_1 and G_2 (given by (4) below, for instance). Note that each iteration of (3) is easy to solve, for example using the command `hinfsyn` in MATLAB [12]. Concerning the quality of these subsystems, the following proposition holds.

Proposition 2. *Suppose Assumptions 1-2 hold, and that the recursion* (3) *is initialized with*

$$\begin{aligned} \hat{G}_1^{(0)} &:= \arg \min_{\hat{G}_1 \in \mathcal{RH}_\infty} \|\lambda_1(H_1 - F_1 \hat{G}_1)\|_\infty, \\ \hat{G}_2^{(0)} &:= \arg \min_{\hat{G}_2 \in \mathcal{RH}_\infty} \gamma(\hat{G}_1^{(0)}, \hat{G}_2). \end{aligned} \tag{4}$$

Then for all $k \geq 0$,

$$0 \leq \gamma(\hat{G}_1^{(k+1)}, \hat{G}_2^{(k+1)}) \leq \gamma(\hat{G}_1^{(k)}, \hat{G}_2^{(k)}) \leq 2\epsilon(1 + \|(\lambda_2 F_2/\lambda_1 F_1) G_2^\star\|_\infty).$$

Using the convex relaxation, we can again converge to a local minimum. But from Proposition 2, we get a worst-case bound on the reconstruction error. The distance from the cascade of $\hat{G}_1^{(0)}$ and $\hat{G}_2^{(0)}$ to H is at most $2\epsilon(1 + \|(\lambda_2 F_2/\lambda_1 F_1) G_2^\star\|_\infty)$, and further iterations can not increase the distance. The bound is expected to be a quite conservative because it is derived using the sub-multiplicative property of the $\mathcal{L}_\infty$-norm. Nevertheless, we see from the bound that if there exists a cascade system that very accurately models H, *i.e.* there is a very small ϵ that renders Assumption 2 true, then already $\hat{G}_1^{(0)}$ and $\hat{G}_2^{(0)}$ will be good estimates. As we shall see in the numerical studies in Section 5, the convex relaxation performs very well in practice and typically converges fast. Let us also note that it may be beneficial to use the output of the convex relaxation as starting point for the earlier mentioned non-convex methods [10].

Remark 1. *Note that one does not need to fix* ϵ *before applying either of the above methods. After a cascade system* $\hat{G}_1, \hat{G}_2 \in \mathcal{RH}_\infty$ *has been found, using either method, one can compute* $\gamma(\hat{G}_1, \hat{G}_2)$. *Since we have now found a cascade system with reconstruction error* $\gamma(\hat{G}_1, \hat{G}_2)$, *we can safely assume that there is an* $\epsilon \leq \gamma(\hat{G}_1, \hat{G}_2)$. *In the following, we typically choose* $\epsilon = \gamma(\hat{G}_1, \hat{G}_2)$. *It then remains to estimate the corresponding minimal orders* $n_1^\star$ *and* $n_2^\star$.

The presented methods deliver subsystems $\hat{G}_1$ and $\hat{G}_2$ achieving some accuracy $\gamma(\hat{G}_1, \hat{G}_2)$. A potential problem is that these subsystems may be of high order. The orders emanating from (3)–(4) are typically $\deg \hat{G}_1 = 2\deg\lambda_1 + \deg H_1 + \deg F_1$ and $\deg \hat{G}_2 = 2\deg\lambda_1 + 2\deg\lambda_2 + \deg H_1 + \deg H_2 + \deg F_1 + \deg F_2$. Therefore there is a need for model reduction that preserves the accuracy (1). This is the topic of the next section.

4. Model Reduction of Cascade Systems

Based on the results of Section 3, we may assume a cascade system with acceptable reconstruction error has been found, but that its order is too high. Following the discussion in Remark 1, we make the following assumption.

Assumption 3. *$\hat{G}_1, \hat{G}_2 \in \mathcal{RH}_\infty$ of orders n_1 and n_2, respectively, satisfy $\gamma(\hat{G}_1, \hat{G}_2) \leq \epsilon$. Furthermore, $\hat{G}_1$ has no zeros on the unit circle ($|z| = 1$).*

The model reduction problem we are facing next is inherently a frequency-weighted one: the input to the second subsystem $\hat{G}_2$ is filtered through the first subsystem $\hat{G}_1$, as an example. Hence, how well we model H_1 influences how well we can model H_2 with a cascade system. Let us therefore consider the following two frequency-weighted approximation criteria, where G_1 and G_2 denote the sought-after low-order subsystems,

$$\begin{aligned} \left\| \begin{bmatrix} \lambda_1 F_1 \\ \lambda_2 F_2 \hat{G}_2 \end{bmatrix} (\hat{G}_1 - G_1) \right\|_\infty &= \|W_1(\hat{G}_1 - G_1)\|_\infty, \\ \|\lambda_2 F_2 \hat{G}_1 (\hat{G}_2 - G_2)\|_\infty &= \|W_2(\hat{G}_2 - G_2)\|_\infty. \end{aligned} \tag{5}$$

Here $W_1, W_2, W_1^{-1}, W_2^{-1} \in \mathcal{RH}_\infty$ are stable and minimum-phase spectral factors satisfying

$$\begin{aligned} W_1^\sim W_1 &= (\lambda_1 F_1)^\sim (\lambda_1 F_1) + (\lambda_2 F_2 \hat{G}_2)^\sim (\lambda_2 F_2 \hat{G}_2), \\ W_2^\sim W_2 &= (\lambda_2 F_2 \hat{G}_1)^\sim (\lambda_2 F_2 \hat{G}_1). \end{aligned} \tag{6}$$

Under Assumptions 1 and 3, W_1 and W_2 exist since the involved transfer functions are bounded and non-zero on the unit circle, see [5, Theorem 21.27]. The weighted criteria (5) are measures of the approximation error, as sensed in the filtered outputs y_1 and y_2. That is, the first criterion measures the error when we replace $\hat{G}_1$ with G_1, and the second criterion similarly measures the error when we replace $\hat{G}_2$ with G_2.

Following [3, 6], the so-called *weighted Hankel singular values* $\sigma_i(\tilde{W}_1\hat{G}_1)$ and $\sigma_i(\tilde{W}_2\hat{G}_2)$ are the relevant Hankel singular values for approximation criteria of the type (5). Here $\tilde{W}_1 := W_1^{\sim}$ and $\tilde{W}_2 := W_2^{\sim}$. We always assume the singular values are sorted in decreasing order, $\sigma_{i+1}(\cdot) \leq \sigma_i(\cdot)$. Since $\tilde{W}_1$ and $\tilde{W}_2$ are in $\mathcal{RH}_\infty^-$ by construction, there are n_1 non-zero singular values $\sigma_i(\tilde{W}_1\hat{G}_1)$ and n_2 non-zero singular values $\sigma_i(\tilde{W}_2\hat{G}_2)$. The weighted singular values $\sigma_i(\tilde{W}_k\hat{G}_k)$ can be obtained by first making a stable/anti-stable decomposition of $\tilde{W}_k\hat{G}_k$, and then by computing the regular Hankel singular values of the extracted stable component [6].

The reason for the relevance of the weighted singular values is the following fundamental lower bound [3, Eq. (3.3)],

$$\sigma_{r_k+1}(\tilde{W}_k\hat{G}_k) \leq \min_{\substack{G_k \in \mathcal{RH}_\infty \\ \deg G_k \leq r_k}} \|W_k(\hat{G}_k - G_k)\|_\infty, \quad k = 1, 2. \tag{7}$$

Hence, no matter how the r_k-th order system G_k is constructed can it ever be more accurate than $\sigma_{r_k+1}(\tilde{W}_k\hat{G}_k)$. In the following lemma, we show how these weighted Hankel singular values are related to the corresponding singular values for the "ideal" cascade system.

Lemma 1. *Under Assumptions 1–3, it holds*

$$\sigma_i(\tilde{W}_k\hat{G}_k) \leq \sigma_i(\tilde{W}_kG_k^\star) + \kappa_k\epsilon, \quad k = 1, 2,$$

with the constants $\kappa_1 = 2+2\|(\lambda_2F_2/\lambda_1F_2)\hat{G}_2\|_\infty$, $\kappa_2 = 2+2\|(\lambda_2F_2/\lambda_1F_2)G_2^\star\|_\infty$, *and where* $\sigma_i(\tilde{W}_kG_k^\star)$ *are zero for* $i > n_k^\star$.

The lemma says that if the reconstruction problem is well posed, *i.e.* there is a small ϵ that renders Assumptions 2–3 true, then $\sigma_i(\tilde{W}_k\hat{G}_k)$ are small as soon as i is larger than the order of the "ideal" solution $G_k^\star$. Hence, the weighted singular values are good indicators of suitable model order for the cascade system.

Next, we discuss how to actually make the criteria (5) small and close to the lower bound (7). Several options exists for this, see, *e.g.* [6]. Balanced truncation and its generalization was used on a related problem in [9]. Here we prefer frequency-weighted optimal Hankel-norm approximation, see, *e.g.* [3, 6], since it comes with an upper error bound expressed in the weighted Hankel singular values, see [4]. In fact, this method systematically yields r_k-th order approximations G_k satisfying

$$\|W_k(\hat{G}_k - G_k)\|_\infty \leq \nu_k \sum_{i=r_k+1}^{n_k} \sigma_i(\tilde{W}_k\hat{G}_k), \quad k = 1, 2, \tag{8}$$

for some computable constants ν_1 and ν_2, see [4] and the proof of Theorem 1 below. In particular, we see that if the singular values for $i = r_{k+1}, \ldots, n_k$ are small, then G_k is necessarily an accurate approximation.

Using frequency-weighted optimal Hankel-norm approximation on the estimated models $\hat{G}_1$ and $\hat{G}_2$, we obtain the following bounds on the reconstruction error.

Theorem 1. *Suppose Assumptions 1 and 3 hold. Let $G_1, G_2 \in \mathcal{RH}_\infty$ be r_1-th and r_2-th order weighted optimal Hankel-norm approximations of $\hat{G}_1$ and $\hat{G}_2$, respectively. Then there are positive constants ν_1 and ν_2, depending solely on W_1 and W_2, such that*

$$\sigma_{r_1+1}(\tilde{W}_1\hat{G}_1) - \epsilon \leq \gamma(G_1, \hat{G}_2) \leq \epsilon + \nu_1 \sum_{i=r_1+1}^{n_1} \sigma_i(\tilde{W}_1\hat{G}_1),$$

$$\sigma_{r_2+1}(\tilde{W}_2\hat{G}_2) - \epsilon \leq \gamma(\hat{G}_1, G_2) \leq \epsilon + \nu_2 \sum_{i=r_2+1}^{n_2} \sigma_i(\tilde{W}_2\hat{G}_2),$$

when we choose r_k, such that $\sigma_{r_k+1}(\tilde{W}_k\hat{G}_k) \geq \epsilon$, for $k = 1, 2$. The upper bounds hold irrespective of r_k.

Remark 2. *There are lower bounds on γ also when $\sigma_{r_k+1}(\tilde{W}_k\hat{G}_k) < \epsilon$: When $\nu_k \sum_{i=r_k+1}^{n_k} \sigma_i(\tilde{W}_k\hat{G}_k)$ is is greater than ϵ, the lower bound is trivial ($= 0$), and otherwise the lower bound is $\epsilon - \nu_k \sum_{i=r_k+1}^{n_k} \sigma_i(\tilde{W}_k\hat{G}_k)$.*

Using the singular values it is therefore possible to *a priori* estimate the effect of replacing the preliminary subsystems from Section 3 with their reduced counterparts. Once the reduced models have been computed, it is possible to compute the actual value of $\gamma(G_1, G_2)$, and so the role of the bounds is to efficiently find reasonable orders r_1 and r_2. Testing all possible combinations of r_1 and r_2 may otherwise be very time consuming. The following corollary is a direct consequence of Theorem 1 and Lemma 1.

Corollary 1. *Suppose Assumptions 1–3 hold. Then*

$$\gamma(G_1, \hat{G}_2) \leq [1 + \nu_1\kappa_1(n_1 - r_1)]\epsilon,$$
$$\gamma(\hat{G}_1, G_2) \leq [1 + \nu_2\kappa_2(n_2 - r_2)]\epsilon,$$

if $n_1 \geq r_1 \geq n_1^\star$ and $n_2 \geq r_2 \geq n_2^\star$.

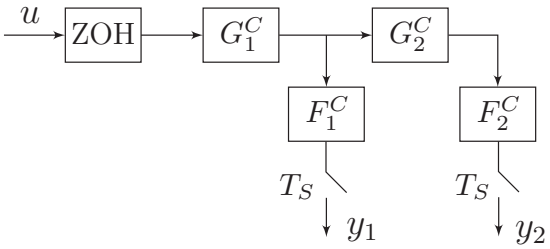

Figure 2: The ZOH sampled continuous-time cascade system considered in Section 5.1.

Hence, if we choose orders for the reduced cascade system that are at least as large as the orders of the "ideal" solutions, and the problem is well posed, then the reconstruction error $\gamma(G_1, G_2)$ will be small. To demonstrate the effectiveness of the proposed methods, we analyze two examples next.

5. Examples

5.1. Sampled Resonant Cascade System

Consider the zero-order-hold (ZOH) sampled continuous-time cascade system in Figure 2. The continuous-time transfer functions are of the form

$$G_k^C(s) = \frac{\omega_k^2(s/\alpha_k + 1)^2}{s^2 + 2\zeta_k\omega_k s + \omega_k^2} \cdot \frac{1 - p_1\tau_k s + p_2(\tau_k s)^2 + \ldots \pm p_{l_k}(\tau_k s)^{l_k}}{1 + p_1\tau_k s + p_2(\tau_k s)^2 + \ldots + p_{l_k}(\tau_k s)^{l_k}}, \quad k = 1, 2,$$

where the coefficients $\{p_i\}_{i=1}^{l_k}$ are from an l_k-th order Padé-approximation[1] of e^{-s}, see, *e.g.* [13]. We use the parameters

$$\begin{aligned} &\omega_1 = 2.0, \quad \zeta_1 = 0.3, \quad \alpha_1 = 5.0, \quad \tau_1 = 0.5, \quad l_1 = 10, \\ &\omega_2 = 5.0, \quad \zeta_2 = 0.1, \quad \alpha_2 = 10, \quad \tau_2 = 1.0, \quad l_2 = 15, \end{aligned}$$

and G_1^C and G_2^C are of orders 12 and 17, respectively. The sampling frequency is $T_S = 0.1$, and the systems F_1^C and F_2^C model anti-aliasing filters, both of orders one. Their bandwidths are chosen to half the Nyquist frequency.

[1]To avoid some numerical issues in later steps, we prefer to use Padé-approximations and work with sampled systems without poles in $z = 0$.

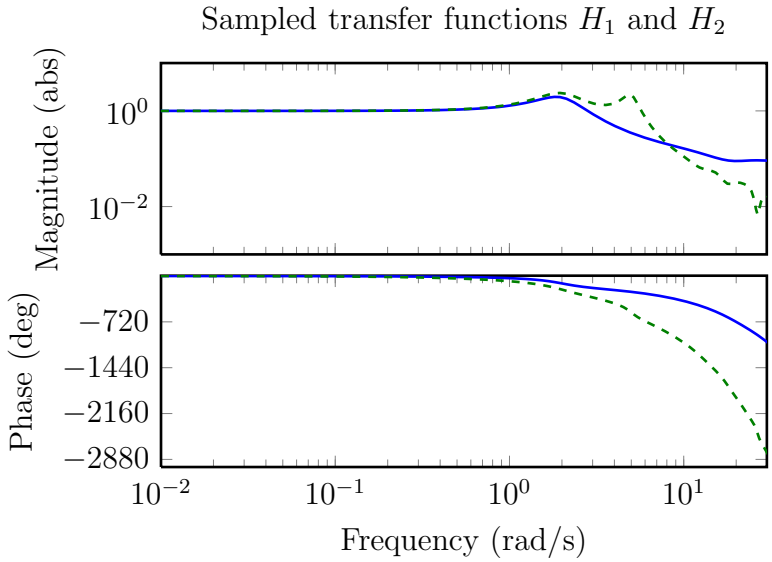

Figure 3: Bode diagrams of the transfer functions H_1 (solid) and H_2 (dashed) in Section 5.1.

This numerical example can be thought of as a cascade of two resonant systems with some additional phase loss. It illustrates that our methods do not require stable system inverses, and can deal with systems of moderate order. A real sampled cascade system, albeit of lower order and with no non-minimum phase components, is considered in Section 5.2.

We note that after ZOH sampling, the sampled transfer functions H_1 and H_2, see Figure 3, are not exactly in cascade form, but closely so because of the underlying continuous dynamics. We next want to recover good discrete-time subsystem estimates G_1 and G_2, along with appropriate model orders. For F_1 and F_2, we simply use matched pole-zero sampling of the continuous-time time equivalents F_1^C and F_2^C.

The next step is to find a preliminary cascade system $\hat{G}_1$ and $\hat{G}_2$, matching H_1 and H_2 (we use $\lambda_1 = \lambda_2 = 1$). We first apply the recursion (3)–(4). The iteration converges immediately at step 0, and we obtain the accuracy $\epsilon = 0.0040$, to be compared with $\|H\|_\infty = 3.07$. As expected, $\mathcal{H}_\infty$ model matching gives high-order solutions, and the obtained $\hat{G}_1$ and $\hat{G}_2$ are of orders $n_1 = 14$ and $n_2 = 45$, respectively. For comparison, we try to solve the original non-convex problem (2) directly using `hinfstruct`. For this,

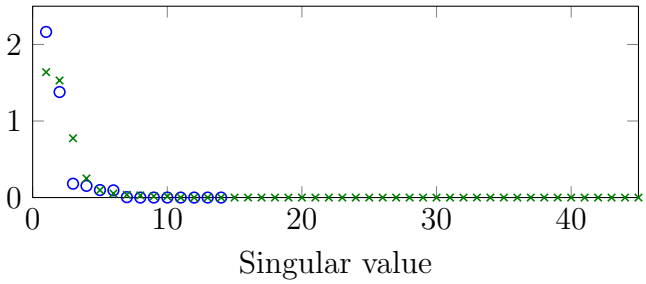

Figure 4: The weighted Hankel singular values $\sigma_i(\tilde{W}_k\hat{G}_k)$ for the two subsystems, $k = 1$ (circle) and $k = 2$ (cross).

we need to estimate good orders for $\hat{G}_1$ and $\hat{G}_2$, and we choose $n_1 = 15$ and $n_2 = 20$ (higher orders lead to slower convergence). From six random starting points, the resulting best accuracy is $\epsilon \approx 0.090$. Clearly the convex relaxation works better here. We choose those estimates for the following order reduction, and therefore $\epsilon = 0.0040$, $n_1 = 14$, and $n_2 = 45$.

We compute the weighted Hankel singular values for the subsystem estimates, see Figure 4. Guided by our derived error bounds, and assuming we can accept an error of around 0.1 in each channel, we choose orders such that $\sigma_{r_k+1}(\tilde{W}_k\hat{G}_k) \approx 0.1$. This leads to the choices $r_1 = r_2 = 4$. These orders are used to construct G_1 and G_2 with optimal weighted Hankel-norm approximation. For comparison, we also use regular optimal (unweighted) Hankel-norm approximation. That is, model reduction that makes the criterion $\|\hat{G}_k - G_k\|_\infty$ small. The reason for this comparison is to check whether it is worth the extra effort to include the weights W_1 and W_2. Finally, we again try to solve the non-convex problem (2) using `hinfstruct`, but this time using the orders $n_1 = n_2 = 4$. As starting points for the non-convex method, we use the output from the weighted Hankel method and another five random points, retaining the best solution. Figures 5–6 illustrate how well the reduced cascade systems are able to approximate H_1 and H_2, for the different methods. It is clear that it is worthwhile to include the weights. Without the weights, the reduced system fails to approximate H_1 and H_2 well for most frequencies. It is interesting to notice that non-convex optimization improves the approximation at many frequencies, but there is no dramatic overall $\mathcal{H}_\infty$ improvement in either channel. It is important to use `hinfstruct` with good estimates of model orders, and the weighted singular

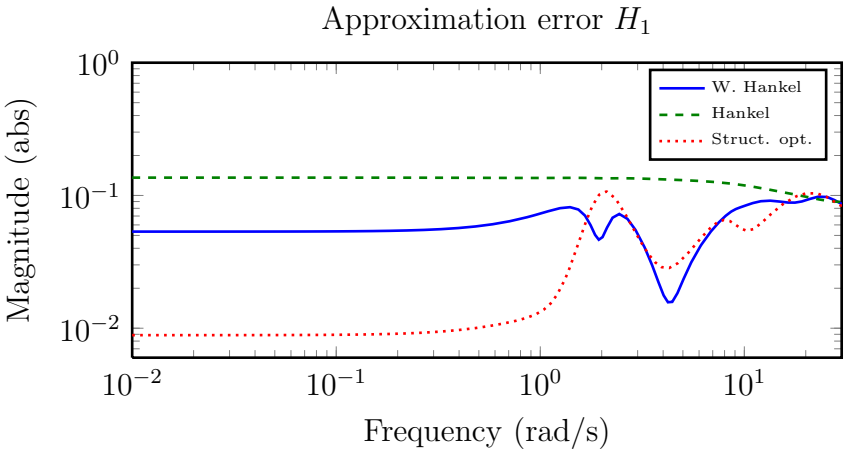

Figure 5: Approximation error $|H_1 - F_1 G_1|$ for the three methods used in Section 5.1 to construct G_1 and G_2: weighted Hankel approximation ('W. Hankel'), regular Hankel approximation ('Hankel'), and non-convex optimization ('Struct. opt.').

values provided such input here. To conclude, we note that indeed the error is around 0.1 in each channel, as predicted by the singular values. Therefore, the models G_1 and G_2 from the weighted Hankel method and the non-convex method must be very close to the true optimal solutions.

5.2. Sampled Double Tank System

Next, we apply the method to a real double tank lab system, see [14] for details. The system consists of two water tanks. A pump driven by a DC-motor pumps water from a water basin into the upper tank. Water then flows, through orifices located in the bottom of each tank, from the upper tank into the lower tank, and from the lower tank into the water basin. The input to the system is the voltage applied to the DC-motor and the outputs are the tank levels in the upper and lower tank, respectively. The sensor outputs are filtered by known low-pass filters, modeled here as $F_1(z) = \frac{0.99}{z-0.01}$ and $F_2(z) = \frac{0.95}{z-0.05}$, respectively. Since the outflows of the two tanks are functions of the water level in the corresponding tank, the system has a cascade structure, as in Figure 2.

The unstructured discrete-time system H is obtained by system identification. A white Gaussian noise process is used as input during the experiment.

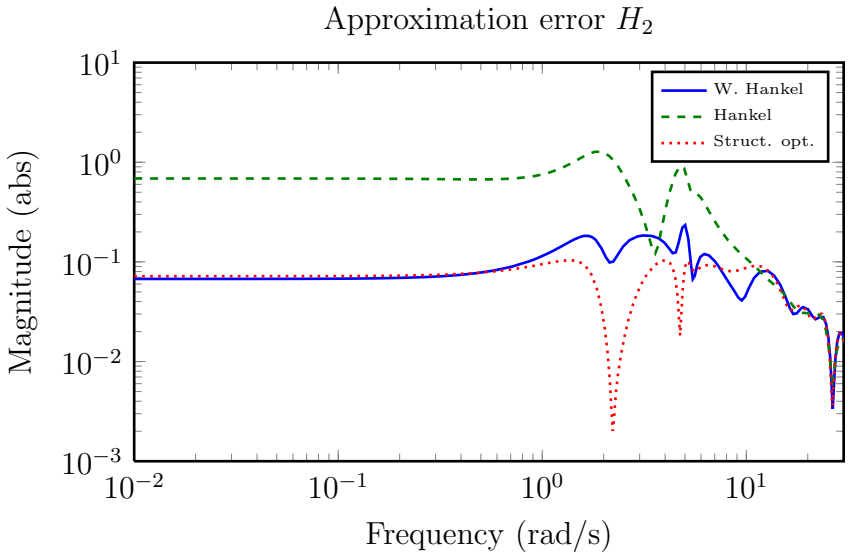

Figure 6: Approximation error $|H_2 - F_2 G_2 G_1|$ for the three methods used in Section 5.1 to construct G_1 and G_2: weighted Hankel approximation ('W. Hankel'), regular Hankel approximation ('Hankel'), and non-convex optimization ('Struct. opt.').

The sampling time is chosen as $T_S = 1$ s and 400 samples of the input and outputs are collected from a real tank process. The models H_1 and H_2 are identified with the subspace identification method `n4sid` [1]. It is possible to directly estimate low-order models with this method but it is often better to estimate high-order models and then apply model reduction, see [8]. The model orders chosen are $\deg H_1 = 6$ and $\deg H_2 = 12$.

The next step is to find high-order estimates $\hat{G}_1$ and $\hat{G}_2$ of the two subsystems from the identified models (using $\lambda_1 = \lambda_2 = 1$). The model matching recursion (3)–(4) is again used. We obtain the model mismatch $\epsilon = 1.6 \cdot 10^{-8}$, which should be compared to the norm of the identified system $\|H\|_\infty = 0.83$. Again the method converges in the first iteration. The orders of the structured models are $n_1 = 7$ and $n_2 = 20$. We also apply non-convex optimization as in Section 5.1, but this does not improve the accuracy here.

The final step is to find the appropriate order and reduce the models $\hat{G}_1$ and $\hat{G}_2$. In Figure 7, the Hankel singular values $\sigma_i(\tilde{W}_k \hat{G}_k)$ are shown for $k = 1, 2$. It is seen that there are large drops after the first singular value for

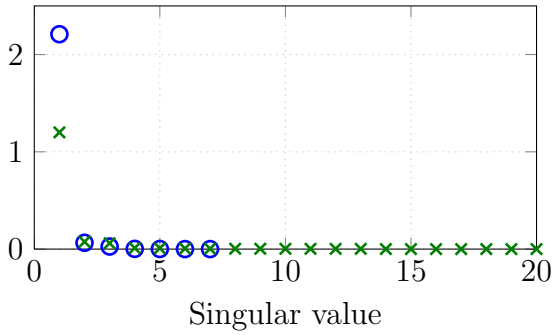

Figure 7: The weighted Hankel singular values $\sigma_i(\tilde{W}_k\hat{G}_k)$ for the two subsystems $k = 1$ (circle) and $k = 2$ (cross).

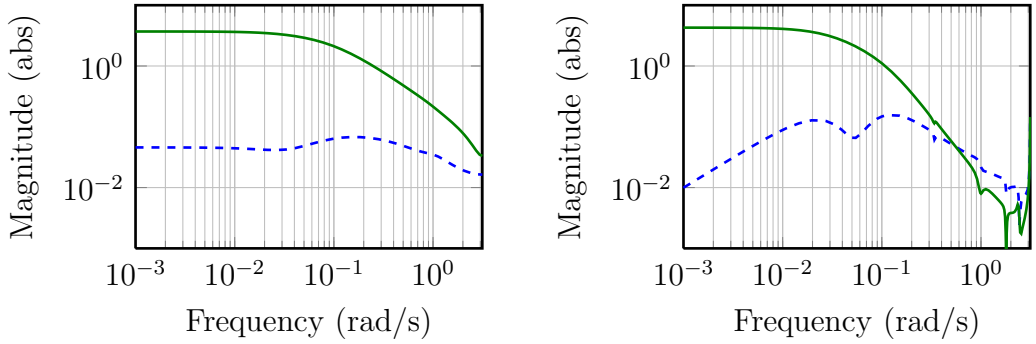

Figure 8: Identified unstructured models $|H_1|$ (left) and $|H_2|$ (right) in solid and approximation errors $|H_1 - F_1G_1|$ (left) and $|H_2 - F_2G_2G_1|$ (right) in dashed.

both subsystems. This is quite expected from Lemma 1, since from physical intuition a single state (the water level) should be enough to model each subsystem. We choose $r_1 = r_2 = 1$ and obtain G_1 and G_2 using weighted Hankel-norm reduction. In Figure 8, the approximation error between the reduced system and the identified model H is shown. It is seen that we have successfully found a low-order cascade system, which approximates the identified models using the developed methods.

6. Convergence Properties

Finally, we prove that the previously presented methods behave well under repeated application on a sequence of systems converging to a true cas-

cade system. That is, we show that the previously introduced constants and weights are bounded, and that we indeed recover the true cascade system in the limit. For this, we need to impose slightly different conditions on the involved systems. In particular, they will belong to $\mathcal{RH}_\infty(\mathbb{C}_a) \subseteq \mathcal{RH}_\infty$, for some $a \in (0, 1]$. This ensures that no poles come closer than $1 - a$ to the unit circle. We will use an $\mathcal{L}_\infty$-norm evaluated on the circle $|z| = a$ and denote it by $\|\cdot\|_{\infty,a}$. Note that by the maximum modulus principle, it holds $\|G\|_\infty \leq \|G\|_{\infty,a}$ if $G \in \mathcal{RH}_\infty(\mathbb{C}_a)$.

Assumption 4. *$G_1^\star, G_2^\star, F_1, F_2, \lambda_1, \lambda_2 \in \mathcal{RH}_\infty(\mathbb{C}_a)$, and F_1, F_2, λ_1, λ_2, and $G_1^\star$ have no zeros on the circle $|z| = a$.*

Assumption 5. *Let*

$$H^\star = \begin{bmatrix} H_1^\star \\ H_2^\star \end{bmatrix} := \begin{bmatrix} F_1 G_1^\star \\ F_2 G_2^\star G_1^\star \end{bmatrix}, \quad \lambda := \mathit{diag}\{\lambda_1, \lambda_2\},$$

where $G_1^\star$ and $G_2^\star$ are of order $n_1^\star$ and $n_2^\star$, respectively. The sequence of systems $\{H^\epsilon\}$, $H^\epsilon \in \mathcal{RH}_\infty(\mathbb{C}_a)$, parameterized by ϵ, is of bounded order and converges to the cascade system $H^\star \in \mathcal{RH}_\infty(\mathbb{C}_a)$, $\|\lambda(H^\star - H^\epsilon)\|_{\infty,a} = \epsilon \to 0$.

Remark 3. *The Assumptions 4–5 replace the Assumptions 1–2. They are slightly stronger in the sense that $\mathcal{RH}_\infty(\mathbb{C}_a) \subseteq \mathcal{RH}_\infty$, and we also require that $G_1^\star$ does not have a zero on the circle $|z| = a$. On the other hand, they are also more flexible in the sense that there is always a circle $|z| = a$ that does not intersect any of the system zeros.*

We have the following result showing that we indeed recover the correct input-output models of the cascade subsystems in the limit.

Theorem 2. *Suppose $a \in (0, 1]$ is chosen such that Assumption 4 holds, and that the sequence $\{H^\epsilon\}$ satisfies Assumption 5. Construct sequences $\{\hat{G}_1^\epsilon\}$ and $\{\hat{G}_2^\epsilon\}$ from the following model matching problems*

$$\begin{aligned} \hat{G}_1^\epsilon &:= \arg \min_{\hat{G}_1 \in \mathcal{RH}_\infty(\mathbb{C}_a)} \|\lambda_1(H_1^\epsilon - F_1 \hat{G}_1)\|_{\infty,a}, \\ \hat{G}_2^\epsilon &:= \arg \min_{\hat{G}_2 \in \mathcal{RH}_\infty(\mathbb{C}_a)} \|\lambda_2(H_2^\epsilon - F_2 \hat{G}_2 \hat{G}_1^\epsilon)\|_{\infty,a}, \end{aligned} \tag{9}$$

where $\hat{G}_1^\epsilon, \hat{G}_2^\epsilon \in \mathcal{RH}_\infty(\mathbb{C}_a)$. Then $\|G_1^\star - \hat{G}_1^\epsilon\|_{\infty,a} \to 0$ and $\|G_2^\star - \hat{G}_2^\epsilon\|_{\infty,a} \to 0$ as $\epsilon \to 0$.

Remark 4. *Note that $\hat{G}_1^\epsilon$ and $\hat{G}_2^\epsilon$ correspond to the subsystems $\hat{G}_1^{(0)}$ and $\hat{G}_2^{(0)}$ from Proposition 2, which initialize the recursion* (3)*. Hence, we have shown that even the initial estimates converge to the true subsystems. Performing more recursions, or solving the full non-convex problem, will obviously converge at least as fast as $\hat{G}_1^\epsilon$ and $\hat{G}_2^\epsilon$.*

Remark 5. *The model matching problems* (9) *can be mapped to standard $\mathcal{H}_\infty$ model matching problems under a transformation $z \mapsto az$ of the complex frequency variable.*

Next, we want to show that when the model reduction method is applied to the sequences $\{\hat{G}_1^\epsilon\}$ and $\{\hat{G}_2^\epsilon\}$, the corresponding weight sequences $\{W_1^\epsilon\}$ and $\{W_2^\epsilon\}$ converges, and the error bound constants $\{\kappa_1^\epsilon\}$, $\{\kappa_2^\epsilon\}$, $\{\nu_1^\epsilon\}$, and $\{\nu_2^\epsilon\}$ are upper bounded. If this were not the case, one may suspect that the reduced-order sequence $\{G_1^\epsilon\}$ and $\{G_2^\epsilon\}$ would not converge to $G_1^\star$ and $G_2^\star$. However, the following proposition shows that the weights and constants are well behaved.

Theorem 3. *Suppose $a \in (0,1)$ is chosen such that Assumptions 4–5 hold. Construct sequences $\{W_1^\epsilon\}$ and $\{W_2^\epsilon\}$ from the following spectral factorization problems*

$$\begin{aligned}(W_1^\epsilon)^\sim W_1^\epsilon &:= (\lambda_1 F_1)^\sim(\lambda_1 F_1) + (\lambda_2 F_2 \hat{G}_2^\epsilon)^\sim(\lambda_2 F_2 \hat{G}_2^\epsilon),\\ (W_2^\epsilon)^\sim W_2^\epsilon &:= (\lambda_2 F_2 \hat{G}_1^\epsilon)^\sim(\lambda_2 F_2 \hat{G}_1^\epsilon),\end{aligned} \tag{10}$$

where $W_1^\epsilon, W_2^\epsilon, (W_1^\epsilon)^{-1}, (W_2^\epsilon)^{-1} \in \mathcal{RH}_\infty$. Then

(i) $\|W_1^\star - W_1^\epsilon\|_\infty \to 0$ and $\|W_2^\star - W_2^\epsilon\|_\infty \to 0$, as $\epsilon \to 0$, where $W_1^\star$ and $W_2^\star$ are defined from (10) *using $\hat{G}_1^\epsilon = G_1^\star$ and $\hat{G}_2^\epsilon = G_2^\star$.*

(ii) The sequences $\{\kappa_1^\epsilon\}$, $\{\kappa_2^\epsilon\}$, $\{\nu_1^\epsilon\}$, and $\{\nu_2^\epsilon\}$ are bounded as $\epsilon \to 0$.

The theorem shows that the model reduction method does not risk the convergence of the reduced models. We have the following corollary by using bounds on the weighted Hankel singular values corresponding to those in Corollary 1.

Corollary 2. *Suppose the orders $r_1 \geq n_1^\star$ and $r_2 \geq n_2^\star$ are used to construct the sequences $\{G_1^\epsilon\}$ and $\{G_2^\epsilon\}$ from $\{\hat{G}_1^\epsilon\}$ and $\{\hat{G}_2^\epsilon\}$ using optimal weighted Hankel-norm approximation. Then $\|G_1^\star - G_1^\epsilon\|_\infty \to 0$ and $\|G_2^\star - G_2^\epsilon\|_\infty \to 0$ as $\epsilon \to 0$.*

7. Conclusion

In this letter, we have proposed and tested model reduction based methods to reconstruct models of cascade systems. We showed how the overall reconstruction error can be bounded in terms of a tolerance parameter ϵ and weighted Hankel singular values. The proposed methods were successfully tested on both a numerical example and a real double tank lab process. We have here used the $\mathcal{H}_\infty$-norm, but it would also be possible to use the $\mathcal{H}_2$-norm. Model matching in the $\mathcal{H}_2$-norm is straightforward [5], and weighted model reduction in the $\mathcal{H}_2$-norm is also possible, see [15]. To develop overall bounds in the $\mathcal{H}_2$-norm is an interesting problem for future work.

Industrial applications often concern system models composed of cascades, feedforward, feedback and multiplicative connections of linear dynamics and memoryless nonlinear elements. For future work, it would also be interesting to develop model approximation techniques for such more general interconnection structures.

Finally, let us note that optimal Hankel-norm approximation and model matching are realistic to apply to systems with a few hundred states. For systems of larger order, one may try to apply approximative methods as described in [16], for example.

Acknowledgments

This work was supported by the Swedish Research Council under grants 2009-4565 and 2013-5523, the European Research Council under the European Community's Seventh Framework Programme (FP7/2007-2013) / ERC Grant Agreement No. 267381, the Swedish Foundation for Strategic Research, and the Linnaeus Center ACCESS at KTH.

Appendix A. Proof of Proposition 2

Let $\Delta_1 := \hat{G}_1^{(0)} - G_1^\star$ and $\Delta_2 := H_2 - F_2 G_2^\star G_1^\star$. From Assumption 2 we know that there are subsystem in the ϵ-neighborhood of H. By using the optimality property of $\hat{G}_1^{(0)}$ and the triangle inequality, we have (i) $\|\lambda_1(H_1 - F_1\hat{G}_1^{(0)})\|_\infty \leq$

ϵ, (ii) $\|\lambda_1 F_1 \Delta_1\|_\infty \leq 2\epsilon$, and (iii) $\|\lambda_2 \Delta_2\|_\infty \leq \epsilon$. It now follows

$$\begin{aligned}\gamma(\hat{G}_1^{(0)}, \hat{G}_2^{(0)}) = \min_{\hat{G}_2 \in \mathcal{RH}_\infty} \gamma(\hat{G}_1^{(0)}, \hat{G}_2) &\leq \epsilon + \|\lambda_2(H_2 - F_2 G_2^\star \hat{G}_1^{(0)})\|_\infty \\ &= \epsilon + \|\lambda_2(\Delta_2 - F_2 G_2^\star \Delta_1)\|_\infty \\ &\leq 2\epsilon + 2\epsilon \|(\lambda_2 F_2)/(\lambda_1 F_1) G_2^\star\|_\infty.\end{aligned}$$

The first inequality follows from (i), the triangle inequality, and that we optimize over all $\hat{G}_2 \in \mathcal{RH}_\infty$ and then $G_2^\star \in \mathcal{RH}_\infty$ is one possible outcome. The second inequality follows by (iii) and the triangle inequality, and then (ii) together with the sub-multiplicative property of the $\mathcal{L}_\infty$-norm.

That $\gamma(\hat{G}_1^{(k+1)}, \hat{G}_2^{(k+1)}) \leq \gamma(\hat{G}_1^{(k)}, \hat{G}_2^{(k)})$ follows since we minimize over $\mathcal{RH}_\infty$ in each iteration. Then $\hat{G}_1^{(k)}$ and $\hat{G}_2^{(k)}$ still are possible solutions in iteration $k+1$, and the objective value will be no worse.

Appendix B. Proof of Lemma 1

First consider an optimal model reduction problem of the ideal system $G_2^\star$, which satisfies [3, Eq. (3.3)] (see also [5, Corollary 19.10] for the continuous-time version),

$$\begin{aligned}\sigma_{r+1}(\tilde{W}_2 G_2^\star) = \min_{G_2 \in \mathcal{RH}_\infty^-(r)} \|W_2(G_2^\star - G_2)\|_\infty \\ = \|W_2(G_2^\star - \bar{G}_2)\|_\infty\end{aligned} \tag{B.1}$$

where $\bar{G}_2 \in \mathcal{RH}_\infty^-(r)$ solves the optimization problem on the first line. Let us turn to the corresponding problem for the found subsystem $\hat{G}_2$,

$$\begin{aligned}\sigma_{r+1}(\tilde{W}_2 \hat{G}_2) = \min_{G_2 \in \mathcal{RH}_\infty^-(r)} \|W_2(\hat{G}_2 - G_2)\|_\infty \\ \leq \|W_2(\hat{G}_2 - \bar{G}_2)\|_\infty \leq \sigma_{r+1}(\tilde{W}_2 G_2^\star) + \|\lambda_2 F_2 \hat{G}_1 (\hat{G}_2 - G_2^\star)\|_\infty,\end{aligned}$$

where the first inequality follows since we optimize over $\mathcal{RH}_\infty^-(r)$ and $\bar{G}_2$ is a possible outcome. The second inequality is simply the triangle inequality. We turn to bounding the last term. Begin by adding and subtracting $\lambda_2 H_2$, and then apply the triangle inequality. This yields

$$\begin{aligned}\|\lambda_2 F_2 \hat{G}_1 (\hat{G}_2 - G_2^\star)\|_\infty &\leq \epsilon + \|\lambda_2(H_2 - F_2 G_2^\star \hat{G}_1)\|_\infty \\ &\leq 2\epsilon + \|\lambda_2 F_2 G_2^\star (G_1^\star - \hat{G}_1)\|_\infty \leq 2\epsilon(1 + \|(\lambda_2 F_2/\lambda_1 F_2) G_2^\star\|_\infty).\end{aligned}$$

Note that in the final step we used $\|\lambda_1 F_1(G_1^\star - \hat{G}_1)\|_\infty \leq 2\epsilon$, which follows from adding and subtracting H_1, and the triangle inequality. This proves the bound on $\sigma_i(\tilde{W}_2\hat{G}_2)$. The bound on $\sigma_i(\tilde{W}_1\hat{G}_1)$ is shown analogously, and one arrives at

$$\begin{aligned}\sigma_{r+1}(\tilde{W}_1\hat{G}_1) &= \min_{G_1 \in \mathcal{RH}_\infty^-(r)} \|W_1(\hat{G}_1 - G_1)\|_\infty \\ &\leq \|W_1(\hat{G}_1 - \bar{G}_1)\|_\infty \leq \sigma_{r+1}(\tilde{W}_1 G_1^\star) + \left\| \begin{bmatrix} \lambda_1 F_1 \\ \lambda_2 F_2 \hat{G}_2 \end{bmatrix} (\hat{G}_1 - G_1^\star) \right\|_\infty .\end{aligned}$$

We turn to bounding the last term,

$$\begin{aligned}\left\| \begin{bmatrix} \lambda_1 F_1 \\ \lambda_2 F_2 \hat{G}_2 \end{bmatrix} (\hat{G}_1 - G_1^\star) \right\|_\infty &\leq \|\lambda_1 F_1(\hat{G}_1 - G_1^\star)\|_\infty + \|\lambda_2 F_2 \hat{G}_2(\hat{G}_1 - G_1^\star)\|_\infty \\ &\leq 2\epsilon + 2\epsilon \|(\lambda_2 F_2/\lambda_1 F_2)\hat{G}_2\|_\infty,\end{aligned}$$

which proves the bound on $\sigma_i(\tilde{W}_1\hat{G}_1)$. Finally, note that (B.1) also implies that $\sigma_i(\tilde{W}_2 G_2^\star) = 0$ when $i > n_2^\star$, since $G_2^\star$ is of order $n_2^\star$ and one can choose $\bar{G}_2 = G_2^\star$. Analogously, it holds that $\sigma_i(\tilde{W}_1 G_1^\star) = 0$ when $i > n_1^\star$. This concludes the proof.

Appendix C. Proof of Theorem 1

We start with proving for the first case. It holds

$$\begin{aligned}\gamma(G_1, \hat{G}_2) &= \left\| \begin{bmatrix} \lambda_1(H_1 - F_1(\hat{G}_1 + G_1 - \hat{G}_1)) \\ \lambda_2(H_2 - F_2\hat{G}_2(\hat{G}_1 + G_1 - \hat{G}_1)) \end{bmatrix} \right\|_\infty \\ &\leq \underbrace{\gamma(\hat{G}_1, \hat{G}_2)}_{\leq \epsilon} + \|W_1(G_1 - \hat{G}_1)\|_\infty .\end{aligned} \tag{C.1}$$

The last term can be upper bounded using [4, Eq. (3.10)]: $\|W_1(G_1 - \hat{G}_1)\|_\infty \leq \underbrace{(1 + \mu(\tilde{W}_1)\|W_1\|_H \|W_1^{-1}\|_2)}_{=\nu_1} \sum_{i=r_1+1}^{n_1} \sigma_i(\tilde{W}_1\hat{G}_1)$. The constant $\mu(\tilde{W}_1)$ is a bound on the ratio between the $\mathcal{L}_\infty$-norm and the $\mathcal{L}_2$-norm of $\tilde{W}_1$ ($\|\tilde{W}_1\|_\infty \leq \mu(\tilde{W}_1)\|\tilde{W}_1\|_2$), and $\|W_1\|_H$ is the Hankel-norm. (It is shown in [4, 17] that $\mu(\tilde{W}_1)$ can be determined solely from the poles of $\tilde{W}_1$.) The upper bound is thereby shown. The lower bound follows from the reverse triangle inequality applied to (C.1).

The bounds on $\gamma(\hat{G}_1, G_2)$ follow completely analogously.

Appendix D. Proof of Theorem 2

Without loss of generality, assume the assumptions are true for $a = 1$. Then

$$\begin{aligned}\|G_1^\star - \hat{G}_1^\epsilon\|_\infty &\leq \left\|\frac{1}{\lambda_1 F_1}\right\|_\infty \|\lambda_1 F_1(G_1^\star - \hat{G}_1^\epsilon) - \lambda_1 H_1^\epsilon + \lambda_1 H_1^\epsilon)\|_\infty \\ &\leq \left\|\frac{1}{\lambda_1 F_1}\right\|_\infty \left(\|\lambda_1(F_1 G_1^\star - H_1^\epsilon)\|_\infty + \|\lambda_1(H_1^\epsilon - F_1\hat{G}_1^\epsilon)\|_\infty\right).\end{aligned}$$

The first term is upper bounded by ϵ and the second term is upper bounded by $2\epsilon(1+\|(\lambda_2 F_2/\lambda_1 F_1)G_2^\star\|_\infty)$ (shown in the same manner as the corresponding bound in Proposition 2). Hence, as $\epsilon \to 0$, the convergence to $G_1^\star$ follows.

The convergence to $G_2^\star$ follows similarly. Note, however, that $\|1/(\lambda_2 F_2 \hat{G}_1^\epsilon)\|_\infty$ needs to be bounded. But this follows since we just showed that $\hat{G}_1^\epsilon$ converges to $G_1^\star$, and $G_1^\star$ has no zeros on the unit circle by assumption.

Appendix E. Proof of Theorem 3

(i): We prove the convergence property for W_2^ϵ next. The weight W_2^ϵ is the spectral factor of $(\lambda_2 F_2 \hat{G}_1^\epsilon)^\sim(\lambda_2 F_2 \hat{G}_1^\epsilon)$. The presumed limiting weight is $W_2^\star$, which is the spectral factor of $(\lambda_2 F_2 \hat{G}_1^\star)^\sim(\lambda_2 F_2 \hat{G}_1^\star)$. Let us define $\Delta := (\lambda_2 F_2)^\sim(\lambda_2 F_2)[(\hat{G}_1^\epsilon)^\sim \hat{G}_1^\epsilon - (G_1^\star)^\sim G_1^\star]$ as the difference between the spectral densities of the sequence under study and its presumed limit. From Theorem 2, we know know that $\|\hat{G}_1^\epsilon - G_1^\star\|_{\infty,a} \to 0$ for the chosen $a \in (0,1)$, and hence

$$\|\Delta\|_{\infty,a} = \|\Delta\|_{\infty,1/a} \to 0, \quad \text{as} \quad \epsilon \to 0. \tag{E.1}$$

The equality $\|\Delta\|_{\infty,a} = \|\Delta\|_{\infty,1/a}$ follows since Δ is parahermitian ($\Delta^\sim = \Delta$). Nevertheless, it is known that spectral factorization is not continuous in $\mathcal{L}_\infty$, see [18], and it is not obvious that the claimed convergence $\|W_2^\epsilon - W_2^\star\|_\infty \to 0$ holds. To prove this, we apply a result from [19].

Consider the Laurent series (see, *e.g.* [20]) of the analytic function $\Delta(z)$,

$$\Delta(z) = \sum_{k=-\infty}^{\infty} c_k z^k, \tag{E.2}$$

where the constant coefficients c_k are given in (E.3) below. The poles of $\Delta(z)$ lie in $\mathbb{D}_a \cup \mathbb{C}_{1/a}$, and then the series converges absolutely, and uniformly, for

all z in the closed annulus $a \leq |z| \leq 1/a$. The coefficients c_k can be computed as,

$$c_k = \frac{1}{2\pi j} \oint_{|z|=r} \frac{\Delta(z)}{z^{k+1}} \, dz, \quad a \leq r \leq 1/a, \tag{E.3}$$

see [20, page 185]. Since the Laurent series converges absolutely for $|z| = 1$, $\Delta(e^{j\omega})$ belongs to the *Wiener algebra* [19, Example 2.4], which is equipped with the norm $\|\Delta\|_W := \sum_{k=-\infty}^{\infty} |c_k| < \infty$. Note that this norm serves as an upper bound on the $\mathcal{L}_\infty$-norm, $\|\Delta\|_\infty = \|\Delta\|_{\infty,1} \leq \|\Delta\|_W$.

We can prove that the coefficients c_k decay exponentially as follows. For $k > 0$, we choose $r = 1/a$ in (E.3) and obtain that $|c_k| \leq a^k \|\Delta\|_{\infty,1/a} = a^k \|\Delta\|_{\infty,a}$. For $k \leq 0$, we choose $r = a$ and obtain $|c_k| \leq a^{-k} \|\Delta\|_{\infty,a}$. Thus for all k, $|c_k| \leq a^{|k|} \|\Delta\|_{\infty,a}$. We now have the following bound on the norm in the Wiener algebra,

$$\|\Delta\|_W = \sum_{k=-\infty}^{\infty} |c_k| \leq \frac{2a}{1-a} \|\Delta\|_{\infty,a}.$$

Therefore, using (E.1) it holds that $\|\Delta\|_W \to 0$ as $\epsilon \to 0$. This is important since [19, Theorem 4.4] shows that the spectral factorization operation is continuous in the Wiener algebra, *i.e.*, $\|W_2^\epsilon - W_2^\star\|_W \to 0$. Since $\|W_2^\epsilon - W_2^\star\|_\infty \leq \|W_2^\epsilon - W_2^\star\|_W$, the claimed convergence holds. A similar argument can now be used to prove convergence of $W_1^\star$.

(ii): From Theorem 2, it follows that κ_1^ϵ is bounded, since $\hat{G}_2^\epsilon$ converges to $G_2^\star$ in the $\mathcal{L}_\infty$-norm, and κ_2^ϵ is already constant for each ϵ.

To show boundedness of ν_1^ϵ, we need to bound $\|W_1^\epsilon\|_H$, $\|(W_1^\epsilon)^{-1}\|_2$, and $\mu(\tilde{W}_1^\epsilon)$ (as defined in the proof of Theorem 1). Since we have convergence of W_1^ϵ to $W_1^\star$ in the $\mathcal{L}_\infty$-norm, and the $\mathcal{L}_\infty$-norm serves as an upper bound on both the Hankel-norm and the $\mathcal{L}_2$-norm, we have convergence of $\|W_1^\epsilon\|_H$ and $\|(W_1^\epsilon)^{-1}\|_2$. The quantity $\mu(\tilde{W}_1^\epsilon)$ is more complicated. It is shown in [4, 17] that $\mu(\tilde{W}_1^\epsilon)$ can be bounded solely based on the pole locations of $\tilde{W}_1^\epsilon$. By Assumption 5 and Theorem 2, the poles of $\tilde{W}_1^\epsilon$ are located in $|z| > 1/a$, and by the bounds in [17, Corollary 3.3], it follows that $\mu(\tilde{W}_1^\epsilon) \leq \sqrt{1 + M\frac{1+a}{1-a}}$, where M is an upper bound on the number of poles of $\tilde{W}_1^\star$, which exists since Assumption 5 requires sequences of bounded order. We can now conclude that ν_1^ϵ is bounded as $\epsilon \to 0$. An analog argument can be applied to ν_2^ϵ. This concludes the proofs.

References

[1] L. Ljung, System Identification - Theory For the User, 2nd ed, Prentice Hall, Upper Saddle River, New Jersey, 1999.

[2] B. Francis, A Course in H^∞ Control Theory, Springer, 1987.

[3] G. A. Latham, B. D. O. Anderson, Frequency-weighted optimal Hankel-norm approximation of stable transfer functions, Systems & Control Letters 5 (4) (1985) 229 – 236. doi:10.1016/0167-6911(85)90014-3.

[4] B. D. O. Anderson, Weighted Hankel-norm approximation: Calculation of bounds, Systems & Control Letters 7 (1986) 247–255.

[5] K. Zhou, J. Doyle, K. Glover, Robust and Optimal Control, Prentice Hall, Upper Saddle River, New Jersey, 1996.

[6] G. Obinata, B. D. O. Anderson, Model Reduction for Control System Design, Springer-Verlag, London, UK, 2001.

[7] B. Wahlberg, On model reduction in system identification, in: Proc. 1986 American Control Conference, 1986.

[8] F. Tjärnström, L. Ljung, L_2 model reduction and variance reduction, Automatica 38 (9) (2002) 1517–1530.

[9] B. Wahlberg, H. Sandberg, Cascade structural model approximation of identified state space models, in: Proceedings of the 47th IEEE Conference on Decision and Control, Cancun, Mexico, 2008.

[10] P. Apkarian, D. Noll, Nonsmooth H_∞ synthesis, Automatic Control, IEEE Transactions on 51 (1) (2006) 71–86. doi:10.1109/TAC.2005.860290.

[11] http://www.mathworks.com/help/robust/ref/hinfstruct.html.

[12] http://www.mathworks.com/help/robust/ref/hinfsyn.html.

[13] http://www.mathworks.com/help/control/ref/pade.html.

[14] K. H. Johansson, The quadruple-tank process: a multivariable laboratory process with an adjustable zero, Control Systems Technology, IEEE Transactions on 8 (3) (2000) 456 –465. doi:10.1109/87.845876.

[15] B. Anić, C. Beattie, S. Gugercin, A. C. Antoulas, Interpolatory weighted-$\mathcal{H}_2$ model reduction, Automatica 49 (5) (2013) 1275 – 1280. doi:http://dx.doi.org/10.1016/j.automatica.2013.01.040.

[16] A. C. Antoulas, Approximation of Large-scale Dynamical Systems, Advances in design and control, Society for Industrial and Applied Mathematics, 2005.

[17] F. De Bruyne, B. D. O. Anderson, M. Gevers, Relating H_2 and H_∞ bounds for finite-dimensional systems, Systems & Control Letters 24 (1995) 173–181.

[18] B. D. O. Anderson, Continuity of the spectral factorization operation, Matematica Aplicada E Computacional 4 (2) (1985) 139–156.

[19] B. Jacob, J. R. Partington, On the boundedness and continuity of the spectral factorization mapping, SIAM J. Control Optim. 40 (1) (2001) 88–106.

[20] L. V. Ahlfors, Complex Analysis, 3rd Edition, International series in pure and applied mathematics, McGraw-Hill, Inc., 1979.